Soft Classification with Gaussian Mixture Model for Clinical Dual-Energy CT Reconstructions

Ruoqiao Zhang, *Student Member, IEEE,* Jean-Baptiste Thibault, *Member, IEEE,*
Charles A. Bouman, *Fellow, IEEE,* and Ken D. Sauer, *Member, IEEE*

***Abstract*—We study the distribution of the clinical dual-energy CT (DECT) reconstructions by applying a soft classification method with Gaussian mixture model. With a pre-described subclass number, this method estimates the parameters of each subclass and performs classification based on the posterior probability. Our study on the clinical data shows that the classification result relates closely to the actual material composition in the human body, with each material represented by a particular cluster. Also, the study shows that the edges in the DECT images follow a Gaussian mixture distribution, where each subclass has a distinguishable covariance or direction that represents a particular type of edges. Potential usage of this soft classification method includes MRF prior design and accurate material separation.**

***Index Terms*—Computed tomography (CT), dual energy, statistical method, Gaussian mixture, material separation, material classification, Markov random field (MRF) design.**

I. Introduction

DUAL-ENERGY CT (DECT) scanners, which collect X-ray projections with two distinct spectra, are of great interest in applications such as disease diagnosis [1] and security inspection [2]. A DECT reconstruction typically produces cross-sections corresponding to the equivalent densities of two basis materials, where the linear combination of the two uniquely determines the energy dependent attenuation [3]. Typical reconstruction approaches include filtered back-projection (FBP) methods and statistical iterative methods. The statistical approaches allow an accurate model for imaging system and detector noise, which consequently reduce the noise and improve the resolution of the images as compared to FBP.

As for statistical iterative reconstruction approaches, it is critical to build an accurate prior model to represent the image characteristics. This requires knowledge of the distribution of the reconstructed quantities. The Markov random field (MRF) has been applied widely in iterative CT reconstruction as a prior model during the recent past [4]–[6]. Conventional MRF priors for single-energy CT only depend on local pixel differences. However, the distribution of the pixel differences in clinical DECT reconstructions remains unclear. Applying the MRF prior to each basis material components separately, as stated in [7], ignores the correlation between different components. Thus, it is necessary to learn the distribution of the pixel differences in clinical DECT reconstructions. Moreover, since the DECT reconstructions may potentially subject to contamination between different material components, it is also beneficial to enforce material separation during the reconstruction. One possible approach is to introduce material density information in the MRF prior, which is neglected in conventional MRF model. This also requires knowledge of the distribution of clinical DECT reconstructions.

In this paper, we study the distribution of the clinical DECT reconstructions by using a soft classification method with Gaussian mixture model. By using this method, we model the distribution of the reconstructions as a mixture of several distinct subclasses, each of which follows a multivariate Gaussian distribution. Given the total number of the subclasses, we estimate the mean, covariance, and prior probability of each subclass. Based on the estimated parameters, we then classify each data point based on the posterior probability. We use the expectation-maximization (EM) algorithm to solve this problem. The classification result on the clinical data reveals the distribution of neighboring pixel differences and pixel densities of the DECT reconstructions.

This soft classification method can also be used to segment the DECT images. DECT has the potential to determine the materials in the scanned object. Previous classification methods generally threshold the reconstructed values to differentiate the materials [8], [9]. In particular, Zamyatin *et al.* [9] applied a Gaussian-based approach after thresholding to simply determine the boundary of the clusters produced by thresholding. These methods substantially depend on predefined thresholds and may not be robust when two distinct clusters overlap extensively. In contrast, the classification method we use in this paper is fundamentally different from what Zamyatin used in [9], since in this soft classification method the prior distribution of each Gaussian is not uniform and the parameters remain unknown before the algorithm starts. The clinical result of the soft classification method shows a desirable segmentation on the DECT images, especially for highly overlapping soft tissues.

II. Methodology

A. DECT reconstruction

We use the joint dual-energy model-based iterative reconstruction (JDE-MBIR) approach [7] to reconstruct basis material densities. The JDE-MBIR method incorporates a

R. Zhang and C. A. Bouman are with the School of Electrical and Computer Engineering, Purdue University, West lafayette, IN 47907-0501 USA (email: zhang393@purdue.edu; bouman@ecn.purdue.edu).

J.-B. Thibault is with GE Healthcare Technologies, Waukesha, WI 53188 USA (email: jean-baptiste.thibault@med.ge.com).

K. D. Sauer is with the Department of Electrical Engineering, University of Notre Dame, Notre Dame, IN 46556-5637 USA (email: sauer@nd.edu).

The author would like to acknowledge GE Healthcare for supporting this work.

quadratic approximation to the polychromatic log-likelihood with an accurate noise model that fully accounts for the statistical dependency in the decomposed sinograms. This approach has been demonstrated to reduce noise and improve spatial resolution as compared to the filtered back-projection (FBP) and other decomposition-based statistical methods that employ decoupled likelihood model [7].

B. Soft classification with Gaussian mixture model

Let $Y = \{Y_n\}_{n=1}^N$ be a sequence of N multivariate random vectors of dimension M. Each Y_n is modeled by the same Gaussian mixture distribution with K subclasses. Each subclass k is specified by the parameters $\theta_k = (\pi_k, \mu_k, R_k)$, defined as the prior probability, mean, and covariance for subclass k, respectively. Furthermore, let X_n be a random variable that determines the subclass label for Y_n. Then, the conditional probability of Y_n given $X_n = k$ and parameter θ is given by

$$p(y_n|k,\theta) = \frac{1}{(2\pi)^{\frac{M}{2}}}|R_k|^{-\frac{1}{2}} \exp\left\{-\frac{(y_n-\mu_k)^t R_k^{-1}(y_n-\mu_k)}{2}\right\}. \tag{1}$$

Then the conditional probability of Y_n given θ is,

$$p(y_n|\theta) = \sum_{k=1}^{K} p(y_n|k,\theta)\pi_k. \tag{2}$$

The log-likelihood of the entire sequence, Y, is then given by,

$$\log p(y|K,\theta) = \sum_{n=1}^{N} \log\left(\sum_{k=1}^{K} p(y_n|k,\theta)\pi_k\right). \tag{3}$$

In this paper, we empirically fix the number of subclasses, K. Then the unknown parameter, θ, can be computed as the maximum-likelihood (ML) estimate given by

$$\hat{\theta} = \arg\max_{\theta} \ \log p(y|K,\theta). \tag{4}$$

Due to the unknown state of the labels, $\{X_n\}_{n=1}^N$, we use the EM algorithm to solve this problem. The EM algorithm works by first estimating $\{X_n\}_{n=1}^N$ by clustering the data, $\{Y_n\}_{n=1}^N$, according to the current subclass parameters, θ. Then it reestimates θ based on this clustering result. This leads to an iterative procedure that alternates between classification and parameter estimation. At the i^{th} iteration, the probability that y_n belongs to subclass k can be computed by using Bayes rule,

$$p(k|y_n,\theta^{(i)}) = \frac{p(y_n|k,\theta^{(i)})\pi_k}{\sum_{j=1}^{K} p(y_n|j,\theta^{(i)})\pi_j}. \tag{5}$$

This gives the classification at the i^{th} iteration. This is a "soft" classification since the membership of y_n to each subclass is represented by a probability. Then based on this classification result, we can update the parameters by maximizing the expectation function,

$$\theta^{(i+1)} = \arg\max_{\theta} E[\log p(y, X|\theta)|y, \theta^{(i)}]. \tag{6}$$

A substitution function approach is used to simplify the computation [10]. The updated parameters for each iteration are given by

$$\bar{N}_k = \sum_{n=1}^{N} p(k|y_n,\theta^{(i)}), \tag{7}$$

$$\pi_k^{(i+1)} = \frac{\bar{N}_k}{N}, \tag{8}$$

$$\mu_k^{(i+1)} = \frac{1}{\bar{N}_k}\sum_{n=1}^{N} y_n p(k|y_n,\theta^{(i)}), \tag{9}$$

$$R_k^{(i+1)} = \frac{1}{\bar{N}_k}\sum_{n=1}^{N}\left(y_n-\mu_k^{(i+1)}\right)\left(y_n-\mu_k^{(i+1)}\right)^T p(k|y_n,\theta^{(i)}). \tag{10}$$

The final classification is computed by

$$\hat{X}_n = \arg\max_{k\in K} \ p(k|y_n,\hat{\theta}). \tag{11}$$

The initial condition can be chosen in the same manner as stated in [10],

$$\pi_k^{(1)} = \frac{1}{K} \tag{12}$$

$$\mu_k^{(1)} = y_l, \text{ where } l = \left\lfloor \frac{(k-1)(N-1)}{(K-1)} \right\rfloor \tag{13}$$

$$R_k^{(1)} = \frac{1}{N}\sum_{n=1}^{N} y_n y_n^t \tag{14}$$

where $\lfloor\cdot\rfloor$ takes the greatest smaller integer. Notice that the initial condition does not require any knowledge of each subclass.

C. Data Formulation

We proposed two different formulations of the reconstructed values to study the distribution of a single pixel and its neighbors.

1) Material distances within neighboring pixels: We first study the distribution of the material distance that is measured as the difference within the same material between neighboring pixels. More precisely, let m_1 and m_2 be the reconstructed water and iodine density images, respectively. Furthermore, let s and r be the locations of two pixels in the image. Then we formulate the 2D distance vector as

$$y_{\{s,r\}} = (m_{1,s} - m_{1,r}, m_{2,s} - m_{2,r}).$$

We then formulate a sequence y as a collection of all such 2D vectors over the entire 8-neighborhood system, $\mathcal{C}$. The soft classification is performed on y, with the subclass number, K, empirically fixed to 7.

2) Material densities within neighboring pixels: We formulate a 4D vector that includes the material density information of a neighboring pixel pair. More precisely, for a neighboring pair $\{s,r\}$, the data vector is formulated as

$$y'_{\{s,r\}} = (m_{1,s}, m_{2,s}, m_{1,r}, m_{2,r}).$$

The soft classification is performed on y', which is the sequence of all such 4D vectors over $\mathcal{C}$, with K empirically fixed to 10.

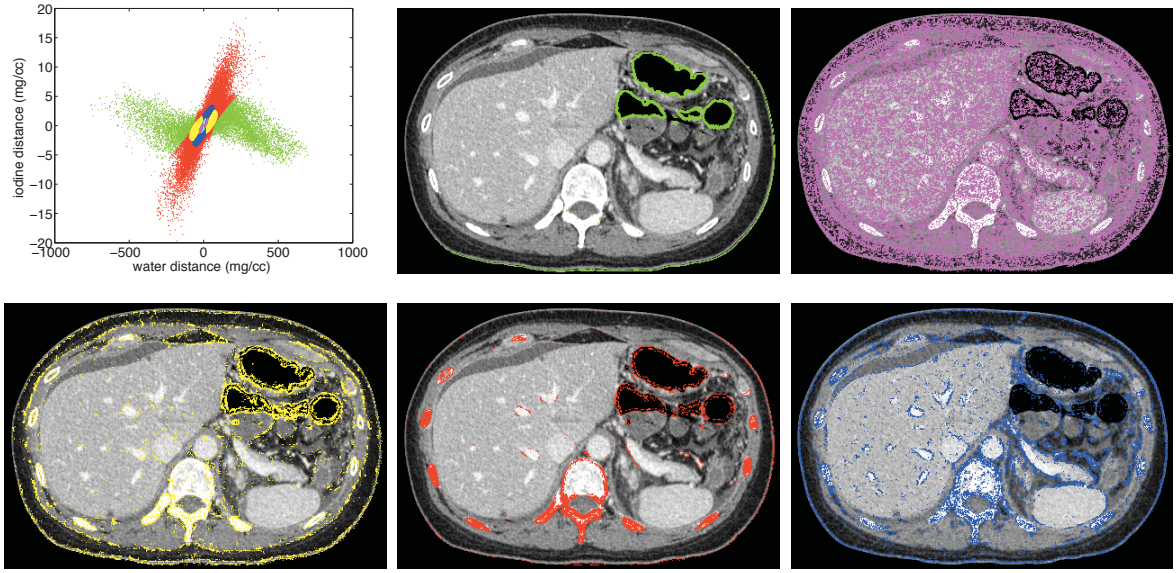

Fig. 1. Classification of the 2D distance vector for FBP images. The scatter-plot shows the classification result, with each color specifying a particular cluster. Then five out of seven subclasses are shown individually on the image, with each represent a particular type of edges. The other two subclasses basically represent DC components and are generally not of great interest.

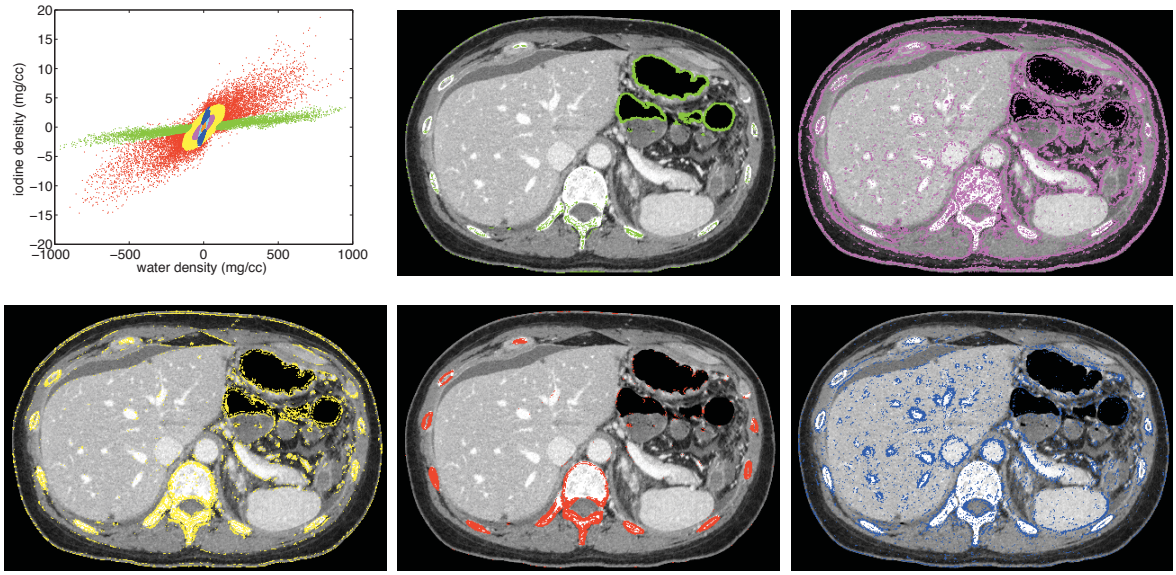

Fig. 2. Classification of the 2D distance vector for JDE-MBIR images. The scatter-plot shows the classification result, with each color specifying a particular cluster. Then five out of seven subclasses are shown individually on the image, with each represent a particular type of edges. The other two subclasses basically represent DC components and are generally not of great interest.

III. Results

We applied the soft classification method on DECT clinical reconstructions. Raw data were acquired on a Discovery CT750 HD scanner (GE Healthcare, WI, USA) in dual-energy fast kVp switching acquisition mode, with tube voltage alternating between 80 kVp and 140 kVp in 540 mAs. We use two methods to reconstruct the water- and iodine-equivalent densities, the FBP method with a standard reconstruction filter kernel and the JDE-MBIR method. We then experimented with the same slice reconstructed by different methods, where the data y and y' were formulated in the manner described in Sec. II-C. We applied the soft classification on y and y' separately.

Fig. 1 and 2 show the classification results on the 2D distance vectors for FBP and JDE-MBIR, respectively. The color-code remains the same for the scatter-plot and the images and the same for FBP and JDE-MBIR cases as well. The results show that the clusters correspond to different types of edges in the images. The clusters have zero mean but different covariances or directions from each other. This suggests an MRF prior that models the distribution of each edge cluster such that different edges can be treated in different ways based on their covariances.

It is also shown in the scatter-plots in Fig. 1 and 2 that

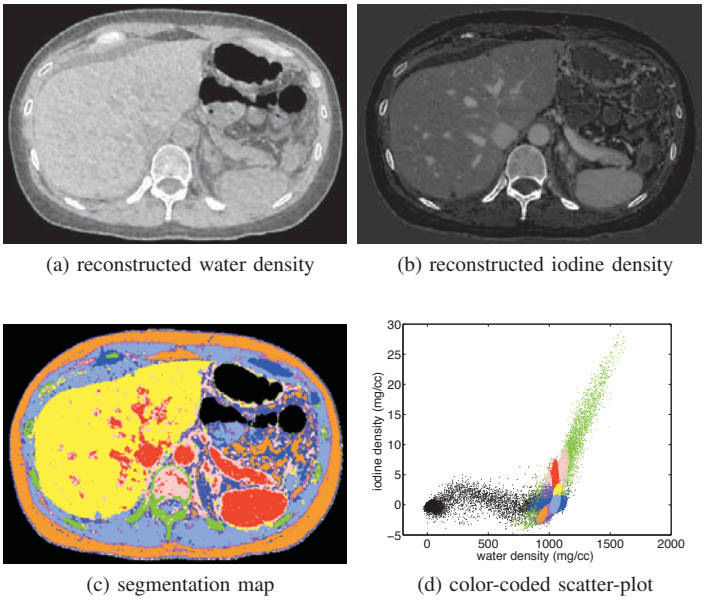

(a) reconstructed water density (b) reconstructed iodine density

(c) segmentation map (d) color-coded scatter-plot

Fig. 3. Classification of the 4D density vector for FBP images. Upper row shows the material density images used in the classification. The classification result is shown on the segmentation map on lower left, with each color specifying a particular cluster. The classification is also shown in the scatter-plot on lower right with the same color code.

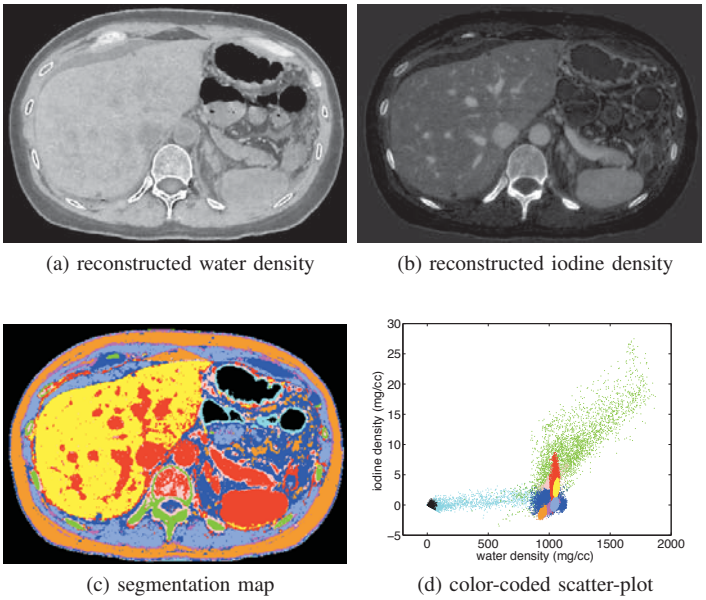

(a) reconstructed water density (b) reconstructed iodine density

(c) segmentation map (d) color-coded scatter-plot

Fig. 4. Classification of the 4D density vector for JDE-MBIR images. Upper row shows the material density images used in the classification. The classification result is shown on the segmentation map on lower left, with each color specifying a particular cluster. The classification is also shown in the scatter-plot on lower right with the same color code.

JDE-MBIR changes the distribution of edges as compared to FBP, where the edges between different material components are positively correlated in JDE-MBIR images. The classification result on the JDE-MBIR images captures and separates different type of edges better than that on the FBP images. As shown in Fig. 2, the high contrast edges (bone-tissue edges (red) and air-tissue edges (green)), and the soft tissue edges (magenta and blue), have been well classified. This is because the JDE-MBIR method produces shaper edges and smoother texture than the FBP method [7].

The classification results of the 4D density vectors are shown in Fig. 3 and 4 for FBP and JDE-MBIR, respectively. Both results show that the clusters relate closely to different compositions of human body, such as fat, muscle, bone, blood, and air. As shown in the images, the soft classification method performs well in differentiating highly overlapping tissues. Moreover, the 4D classification also produces clusters that reflect the edges. For example, the cyan cluster in JDE-MBIR result stands for air-tissue edges. These results indicate the possibility of designing an MRF prior that models both the density distribution and the edge distribution to improve material separation and edge performance simultaneously.

IV. Conclusion

We have presented a study on the distribution of the clinical DECT reconstructions by using a soft classification method with Gaussian mixture model. The soft classification method estimates the parameters of each subclass and performs classification based on the posterior probability. Clinical results have shown that the classification results relate closely to different types of edges in DECT images and different body compositions. Future investigation includes accurate material separation and correlation-based MRF prior design.

References

[1] T. R. Johnson, B. Krauss, M. Sedlmair, M. Grasruck, H. Bruder, D. Morhard, C. Fink, S. Weckbach, M. Lenhard, B. Schmidt, T. Flohr, M. F. Reiser, and C. R. Becker, "Material differentiation by dual energy CT: initial experience," *European J. Radiology*, vol. 17, no. 6, pp. 1510–1517, Jun. 2007.

[2] S. Singh and M. Singh, "Explosives detection systems (EDS) for aviation security," *Signal Process.*, vol. 83, no. 1, pp. 31–55, Jan. 2003.

[3] L. A. Lehmann, R. E. Alvarez, A. Macovski, W. R. Brody, N. J. Pelc, S. J. Riederer, and A. L. Hall, "Generalized image combinations in dual KVP digital radiography," *Med. Phys.*, vol. 8, no. 5, pp. 659–667, Sept./Oct. 1981.

[4] C. A. Bouman and K. D. Sauer, "A generalized Gaussian image model for edge-preserving MAP estimation," *IEEE Trans. Image Process.*, vol. 2, no. 3, pp. 296–310, Jul. 1993.

[5] ——, "A unified approach to statistical tomography using coordinate descent optimization," *IEEE Trans. Image Process.*, vol. 5, no. 3, pp. 480–492, Mar. 1996.

[6] J.-B. Thibault, K. D. Sauer, J. Hsieh, and C. A. Bouman, "A three-dimensional statistical approach to improve image quality for multislice helical CT," *Med. Phys.*, vol. 34, no. 11, pp. 4526–4544, Nov. 2007.

[7] R. Zhang, J.-B. Thibault, C. A. Bouman, K. D. Sauer, and J. Hsieh, "A model-based iterative algorithm for dual-energy X-ray CT reconstruction," in *Proc. 2nd Intl. Mtg. on image formation in X-ray CT*, 2012, pp. 439–443.

[8] N. J. Pelc, "Dual Energy: technical curiosity or potential clinical tool," in *RSNA*, 2007.

[9] A. A. Zamyatin, A. Natarajan, and Y. Zou, "Advanced material separation technique based on dual energy CT scanning," in *Proc. SPIE 7258, Medical Imaging 2009: Phys. Med. Imag.*, vol. 7258, 725844, 2009.

[10] C. A. Bouman. (1997, April) Cluster: An unsupervised algorithm for modeling Gaussian mixtures. [Online]. Available: http://www.ece.purdue.edu/∼bouman